

CALORIMETRIC THERMAL-VACUUM PERFORMANCE CHARACTERIZATION OF THE BAe 80K SPACE CRYOCOOLER

V. Y. Kotsubo, D. L. Johnson and R. G. Ross, Jr.

Jet Propulsion Laboratory
California Institute of Technology
Pasadena, California 91109

ABSTRACT

A comprehensive characterization program is underway at JPL to generate test data on long-life, miniature Stirling-cycle cryocoolers for space application. The key focus of this paper is on the thermal performance of the British Aerospace (BAe) 80K split-Stirling-cycle cryocooler as measured in a unique calorimetric thermal-vacuum test chamber that accurately simulates the heat-transfer interfaces of space. Two separate cooling fluid loops provide precise individual control of the compressor and displacer heatsink temperatures. In addition, heatflow transducers enable calorimetric measurements of the heat rejected separately by the compressor and displacer. Cooler thermal performance has been mapped for coldtip temperatures ranging from below 45 K to above 150 K, for heat-sink temperatures ranging from 280 K to 320 K, and for a wide variety of operational variables including compressor-displacer phase, compressor-displacer stroke, drive frequency, and piston-displacer dc offset.

INTRODUCTION

The recent development of a number of Oxford-heritage, long-life miniature Stirling cryocoolers has led to an explosion of interest in multi-year-life space cryogenic instruments. To assist the space-instrument user community in understanding and applying these important new cryocoolers, the Jet Propulsion Laboratory (JPL) has undertaken a comprehensive program to fully characterize a number of important space cryocoolers with respect to key systems integration and reliability issues¹.

This paper presents the results of a comprehensive study of the thermal performance of the BAe 80K split-Stirling cooler². Previous work on this cooler undertaken at JPL to quantify vibration control³, coldtip parasitics⁴, and EMI compatibility⁵ has been published elsewhere. The thermal performance of the BAe 80K cooler has also been published by other workers⁶, but the present work covers a much more exhaustive set of performance variables and therefore represents the most complete thermal characterization published to date.

Another unique aspect of the JPL testing is the use of a calorimetric thermal-vacuum test facility to simulate

conditions in space and provide a highly stable thermal test environment; the high level of environmental stability achieved allows accurate repeatable measurements to illuminate subtle performance sensitivities that are difficult if not impossible to quantify in typical ambient-room test environments.

The thermal performance of the BAe cooler is presented in terms of both cooling power and specific power (watts of electrical drive power for one watt of cooling power) for a broad range of coldtip temperatures, typically from 150 K down to about 45 K. This performance mapping was conducted parametrically with respect to each of the key environmental and operational variables: heatsink temperature, drive frequency, compressor and displacer stroke, compressor and displacer dc offset, and the phase between the compressor and displacer motions. The ability to individually control the last five parameters is an important feature of the BAe Oxford-heritage cooler; this cooler incorporates independent linear drive motors and displacement transducers in both the compressor and displacer.

The nominal values of the operating parameters used in the testing are shown in Table I.

Table I. Nominal operating parameters used in this study unless otherwise specified

| | |
|----------------------|--------|
| Frequency | 40 Hz |
| Heatsink Temperature | 300 K |
| Compressor Stroke | 7.2 mm |
| Displacer Stroke | 2.6 mm |

TEST APPARATUS AND APPROACH

Figure 1 is a schematic of the thermal vacuum test chamber used for this study. As noted, the compressor and displacer were mounted on separate copper fixtures with separate cooling fluid loops to allow independent control of their heatsink temperatures. The copper fixtures were thermally isolated from the vacuum housing and linked to the fluid loop heat exchangers through heat flow transducers. The heat flow transducers were stainless steel shunts, silver brazed between two long sections of

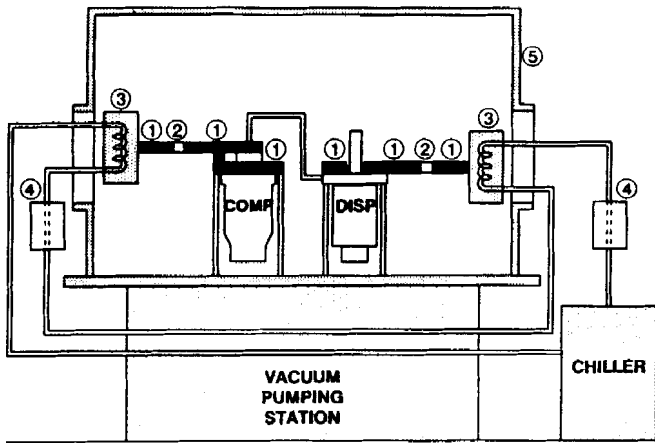


Fig. 1. Schematic of thermal vacuum chamber: 1) copper heatsinks, 2) thermal shunt for heat rejection measurements, 3) fluid-loop heat exchangers, 4) fluid-loop heaters, 5) vacuum bell jar enclosure

copper. Heat from the cooler flowed lengthwise along the copper, through the shunts, then to the heat exchanger, and was quantified by measuring the temperature drop across the shunts.

To calibrate the shunts, metallized Kapton film heaters were bonded to the mounting fixtures and powered at known power levels. To quantify the sensitivity to heat flow uniformity, several foil heaters were attached to various locations on the compressor and displacer fixtures and used to apply different spatial heat distributions. Under worst-case conditions with the same heat input into two widely separated heaters, the results showed less than a 10% variation. The heat flow distribution in the actual test was much more uniform than this worse case, so heat distribution effects can be safely assumed to be negligible. To correct for small parasitic heat leaks, the cooler was operated until steady state was reached, then the temperature drop across the shunts was recorded. The cooler was then turned off, and a measured amount of heater power was applied to match the temperature drop. This provided a direct measure of the cooler heat rejection independent of any parasitic heat leaks from either conduction across the supports or radiation. As a final accuracy check, the total measured heat rejection was compared with the total electrical input power to the cooler; the agreement was always within 1 to 2 watts. In general, the calorimetry worked very well, although the very long thermal equilibration time often required several hours for a single careful calibration.

During the testing, accurate temperature control of the cooler heat sinks was maintained using fluid loops driven by a commercial recirculating chiller; an additional heater in each fluid loop was used to allow individual temperature regulation of the compressor and displacer heatsinks. The system was designed to allow heatsink temperatures from about 220 K to about 330 K, with temperature differences between the compressor and displacer heatsinks of up to 40 K. The large thermal mass of the copper fixtures and coolers helped provide heatsink temperature stability of better than 0.1 K; the temperature of the heatsinks was typically adjusted to within 0.5 K of

the specified temperature. The heatsink temperatures referred to in the data were measured with thermocouples mounted on the copper fixtures immediately adjacent to the cooler-fixture mounting interface. Additional thermocouples mounted at various locations on the compressor indicated that maximum compressor housing temperatures were typically less than 10 K warmer than the heatsink temperature.

To measure the cooler cryogenic performance, the cold tip was outfitted with a cryodiode, and readout was accomplished using commercial electronics with an accuracy of about ± 0.2 K. A 1000-ohm metal film resistor was used to apply a heatload to the coldtip with an accuracy of better than 1%. The coldtip was wrapped in several layers of aluminized Kapton MLI to reduce any parasitic radiation heat load to negligible levels; vacuum levels were typically less than 10^{-5} torr to avoid gaseous conduction effects.

The cooler was driven using a low distortion audio amplifier and waveform synthesizer. The electronic drive system was configured such that the displacements of the compressor and displacer, the dc offsets, the drive frequency, and the compressor-displacer phase could all be individually controlled. The power to the cooler was monitored using high-quality commercial true RMS power meters. Because drive-cable ohmic losses were included in the measurements, a correction for this was subtracted from the compressor power; this was always less than 0.5 W. The displacer drew negligible amounts of current, so no corrections were necessary in the displacer power measurements.

The positions of the compressor piston and displacer were monitored by LVDTs that are an integral part of the cooler construction. The phase between the compressor and displacer motions was measured with a spectrum analyzer to within about 1 degree.

MEASURED SENSITIVITY TO COOLER THERMAL ENVIRONMENT

This section presents a comprehensive mapping of the performance sensitivity of the BAe 80K cooler to heatsink temperature and coldtip thermal load. In the gathering of the performance data, a measured amount of power was applied to the coldtip heater, and as the coldtip equilibrated to its steady state temperature, the drive electronics and the fluid loop temperatures were adjusted to keep the operating parameters at the targeted values. Data were recorded only after the coldtip temperature remained constant for several minutes to ensure that steady state conditions were reached. Typical drive power was on the order of 30 watts (12 volts at 2.5 amps) for the compressor, and typically less than 0.2 W (2 volts at 0.1 amp) for the displacer; under certain conditions, the displacer linear motor actually generated a small amount of (negative) power.

HEATSINK TEMPERATURE- Heatsink temperature is one of the most important external variables in cryocooler operation in that it directly enters into the Carnot efficiency of the cryocooler. Sensitivity to heat sink temperature was measured over the range 280 K to 320 K (7 to 47°C)

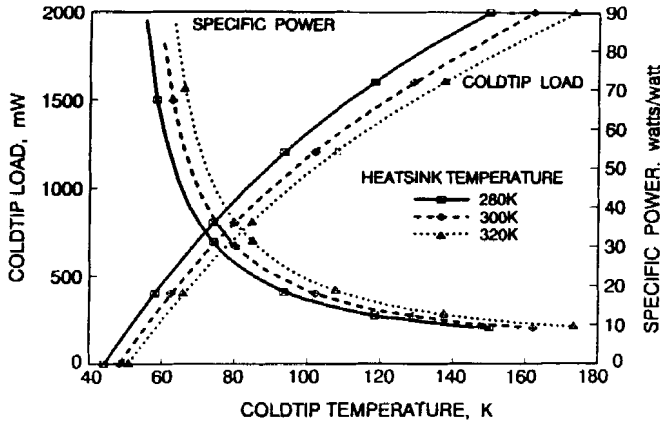


Fig. 2. Thermal performance versus heatsink temperature (displacer same temperature as compressor)

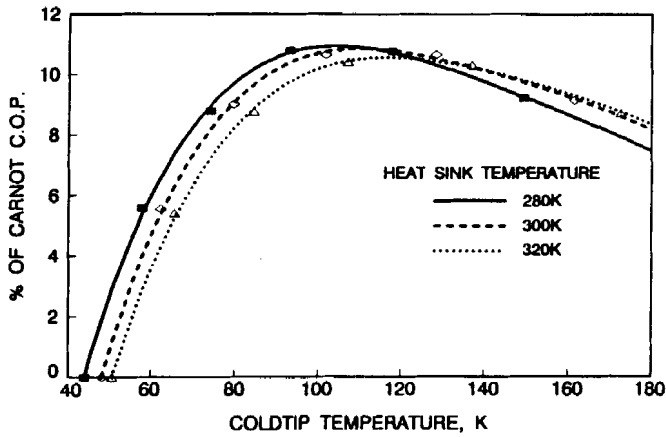


Fig. 3. Cooler efficiency as a percent of Carnot efficiency for various coldtip and heatsink temperatures

--a typical flight allowable operating temperature range-- and is presented in Fig. 2. In this case both the compressor and displacer heatsinks were always kept at the same temperature. The performance is found to improve with colder heatsink temperatures with a coldtip temperature decrease (for constant stroke) of 0.26 K per degree heatsink temperature decrease at ~80 K. For the same 80-K coldtip temperature, the specific power decreases from 29 watts/watt to 27.6 watts/watt as the heatsink temperature is decreased from 300 K to 280 K, and increases to 29.8 watts/watt as the heatsink temperature is increased to 320 K.

An important figure of merit for cryocoolers is the fraction (f) of ideal Carnot efficiency achieved; this fraction Carnot COP is defined as:

$$f = (1/\text{specific power})/[T_c/(T_h - T_c)] \quad (1)$$

where T_c is the coldtip temperature and T_h is the heatsink temperature. Figure 3 plots (f) as computed using the data in Fig. 2. The values, around 10% over most of the operating range, are typical for this type of cooler.

It is interesting to note that for a fixed stroke and coldtip load, if the heatsink temperature is varied and a new coldtip temperature (T_c') is established, (f) remains approximately constant. Because of this, the curves in Fig. 2, to a good approximation, simply translate along the

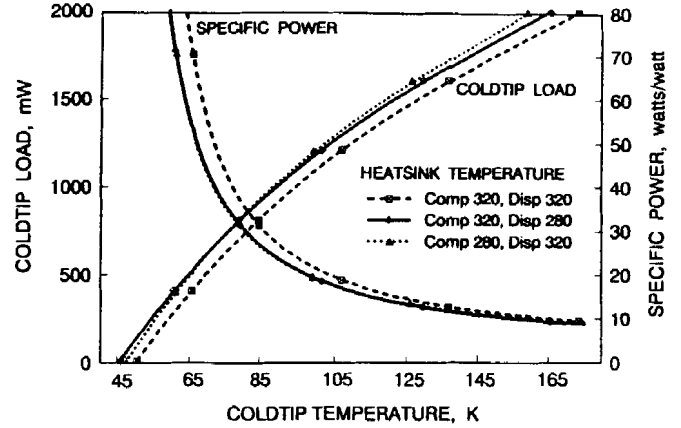


Fig. 4. Effect of unequal compressor-displacer heatsink temperatures on thermal performance

temperature axis as predicted by the Carnot equation, i.e.

$$T_c'/(T_h' - T_c') = T_c/(T_h - T_c) \quad (2)$$

Figure 4 describes the effects of separate displacer and compressor heatsink temperature variations. Notice that the compressor and displacer heatsink temperatures have almost identical effects on cooler performance--each having half the effect noted in Fig. 2 for uniform temperature changes to both heatsinks.

HEAT REJECTION DISTRIBUTION- Although nearly all of the electrical power is input to the compressor, a significant fraction of the resulting thermal energy is known to be passed to the displacer via the transfer tube and is rejected there. Accurately quantifying the distribution of heat rejection between the compressor and displacer is very important for most cryogenic instruments because the compressor and displacer generally have separate heat conduction paths. The displacer heat rejection can be particularly critical for designs where the displacer is supported off of a cryogenically cooled optical bench; in such designs the displacer heat must either be absorbed by the optical bench cooler, or separately conducted back to the overall instrument heatsink.

The calorimetric features of the test chamber were used to map the compressor-displacer heat rejection distribution for a variety of heatsink temperatures and coldtip loads. Figure 5 shows the heat rejected by the compressor and displacer. The curves labeled "compressor" and "displacer" are actual heat rejection measurements, while the curves labeled "total" are the measured total electrical input power, which includes compressor drive power, displacer drive power, and coldtip load. The measured heat rejection agreed well with the total input power, providing a consistency check on the measurement technique. For this case where the compressor and displacer heatsinks have the same temperatures, even with a wide variation in drive parameters, the displacer heat rejection was nearly constant at approximately 6 watts; with equal heatsink temperatures, only the compressor was found to vary in power dissipation with changing operating state.

The one variable that was found to have a significant effect on heat rejection distribution was differences

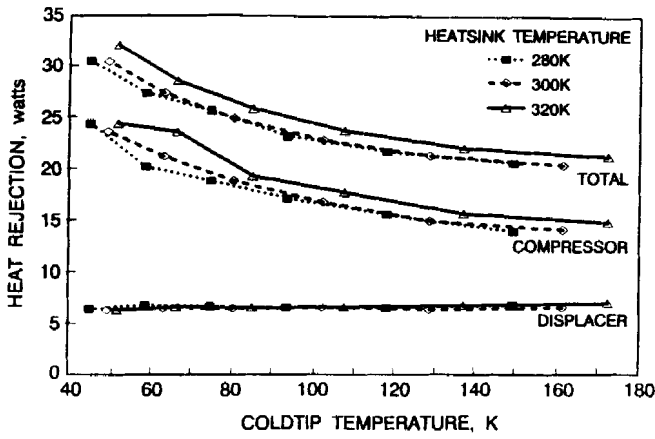


Fig. 5. Heat rejection distribution with compressor and displacer at same heatsink temperatures

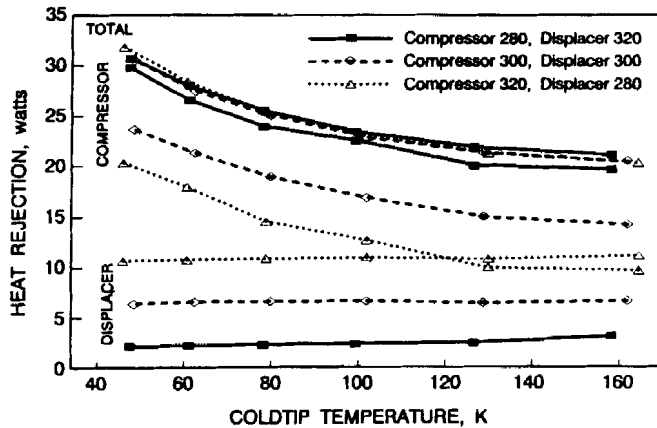


Fig. 6. Heat rejection distribution with compressor and displacer at unequal heatsink temperatures

between the compressor and displacer heatsink temperature. Shown in Fig. 6 is the heat rejection distribution for the same heatsink temperature variations included in Fig. 4. Note that the heat dissipation shifts toward whichever component is colder; when the compressor is 40°C colder than the displacer all but 1 to 2 watts of the heat is dissipated by the compressor. This heat-dissipation shift between the compressor and displacer was found to be linearly proportional to the temperature difference between the two for temperature differences up to $\pm 40^\circ\text{C}$; for temperature differences in this range, the heat shift toward the colder unit is equal to about 0.11 watts/ $^\circ\text{C}$.

MEASURED SENSITIVITY TO COOLER DRIVE VARIABLES

Presented in this section is a comprehensive mapping of the sensitivity of the thermal performance of the BAE 80K cooler to the key externally controllable drive parameters. These parameters include phase between the compressor and displacer, compressor and displacer stroke, drive frequency, and compressor and displacer dc offsets. To provide useful sensitivity data, only one parameter at a time was varied while the others were held at their nominal operating values. The only exception was the phase, which was always set at a value that gave the lowest temperature for the particular operating condition.

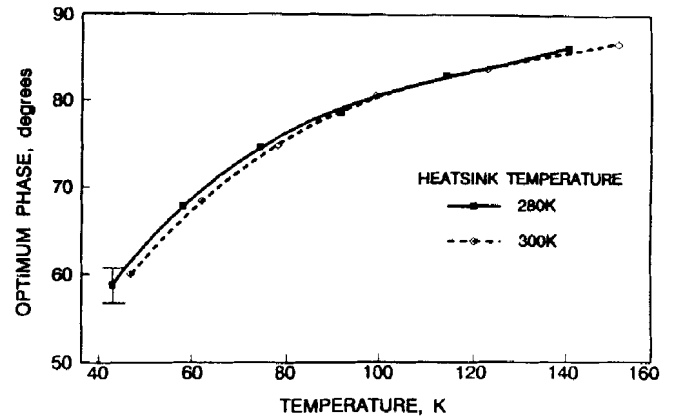


Fig. 7. Optimum phase as a function of coldtip temperature for two heatsink temperatures

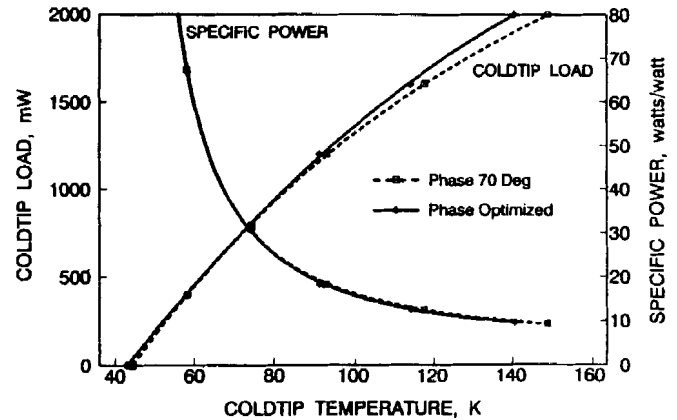


Fig. 8. Performance with phase optimized at each operating point versus a fixed 70° nominal value

COMPRESSOR-DISPLACER PHASE- For a fixed set of drive parameters and coldtip heatload there is an optimum phase between the compressor and displacer motions that results in maximum cooling power; the nominal value of this phase difference is approximately 70°. The sensitivity study to variations in phase was conducted for each operating condition by adjusting the phase until the lowest coldtip temperature was reached. As the compressor stroke, as opposed to input power, is held constant, this procedure does not necessarily optimize the specific power. However, tests have shown that there is only a slight difference in the resulting optimized phases.

Shown in Fig. 7 are the optimum phases for coldtip temperatures between 40 K and 150 K, for heatsink temperatures of 280 K and 300 K. The corresponding coldtip loads and specific powers are shown in Fig. 8. For comparison, the performance curves for the nominal operating phase of 70 degrees is also shown; note that only a slight increase in the cooling capacity is observed when the phase is optimized. Although not distinguishable in this plot, the specific power also decreases slightly with phase optimization beyond the 70° nominal value; the maximum decrease is about 3% for temperatures in the range 55 K to 150 K. Figure 9 demonstrates the insensitivity of the coldtip temperature to phase with no applied coldtip heat load. Near the minimum, a change in the phase of about

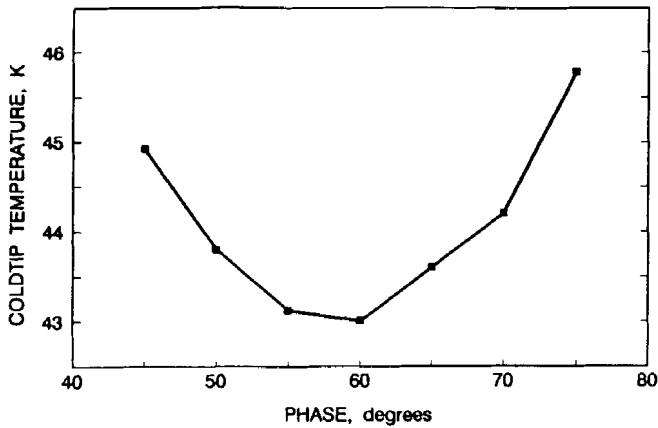


Fig. 9. Sensitivity of the no-load coldtip temperature to phase between compressor and displacer

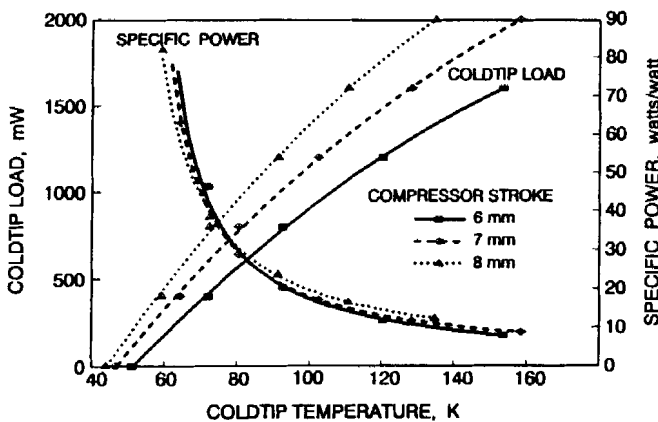


Fig. 10. Performance curves for compressor peak-to-peak strokes of 6 mm, 7 mm, and 8 mm

5 degrees results in only about a 0.2 K change in coldtip temperature. This temperature versus phase behavior was found to be similar at all temperatures, with a slight decrease in the width of the minimum for higher coldtip temperatures.

COMPRESSOR-DISPLACER STROKES- Compressor stroke is the key user controllable variable for varying cooling power and temperature. Figure 10 shows the performance sensitivity for compressor peak-to-peak strokes of 6 mm, 7 mm, and 8 mm. The corresponding swept volumes, as determined by the peak-to-peak stroke times the piston area, were 1.2 cm³, 1.4 cm³, and 1.6 cm³, respectively. Note that the specific power is relatively insensitive to stroke; for temperatures below about 75 K, longer strokes give slightly lower specific power, while above 75 K, longer strokes give slightly higher specific power. In general, as the compressor stroke is increased, the decrease in coldtip temperature and increase in power consumption was found to be quite linear.

Figure 11 shows the performance for displacer peak-to-peak strokes of 2.1 mm, 2.5 mm, and 2.9 mm. The corresponding total swept volumes are 0.17 cm³, 0.20 cm³, and 0.23 cm³. Note that the displacer specific power reaches a minimum at longer strokes, and suggests that a stroke around 3 mm can provide improved performance

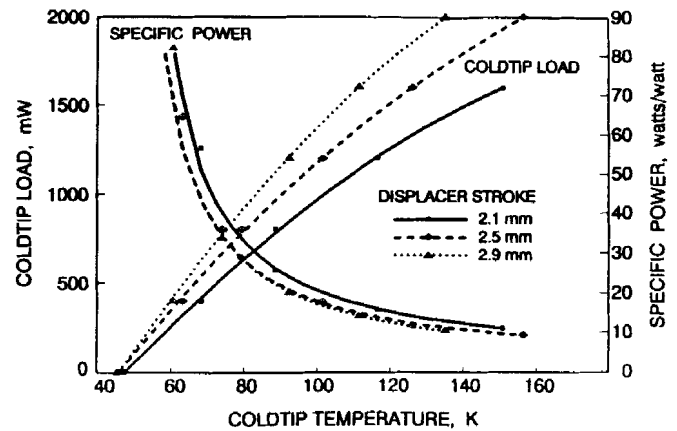


Fig. 11. Performance curves for displacer peak-to-peak strokes of 2.1 mm, 2.5 mm, and 2.9 mm

over the 2.6-mm baseline noted in Table I. Like the compressor, as the displacer stroke is increased, the decrease in coldtip temperature and increase in power consumption was found to be close to linear.

FREQUENCY- Frequency, like compressor stroke, is another key parameter influencing the cooling power of the cryocooler. However, this variable must be treated with caution because frequencies different from the manufacturer's recommended drive frequency can excite internal resonances that can potentially damage or shorten the life of the cooler. This sensitivity study should therefore be viewed as an investigation to understand the fundamentals underlying the cooler operation, not as an incentive to operate the BAE cooler at frequencies other than 40 Hz. Of particular interest to cooler designers is the tradeoff between maximizing compressor drive motor efficiency by operating the compressor at its resonant frequency, maximizing thermal efficiency in the cold end by keeping the frequency lower, or selecting a higher frequency that yields maximum cooling power for a given stroke.

Figure 12 presents the performance sensitivity of the BAE 80K cooler to drive frequency over the range 30 Hz to 50 Hz. The cooling power is seen to increase with increasing drive frequency. Note that the lowest specific power occurs for 40 Hz, which is the manufacturer's recommended operating point. Because different drive

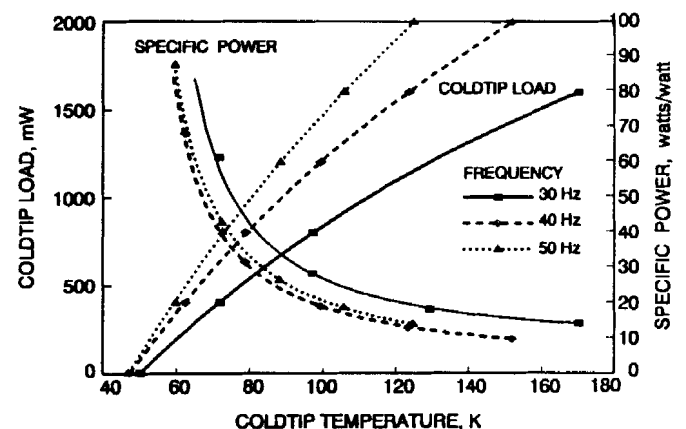


Fig. 12. Performance curve for 30 Hz, 40 Hz, and 50 Hz drive frequencies

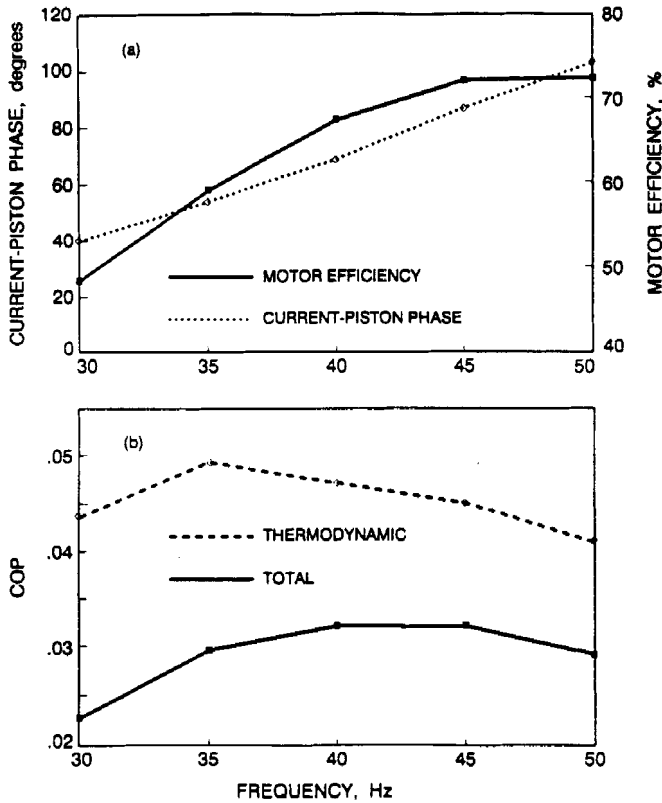


Fig. 13. Frequency sensitivity of cooler performance with coldtip temperature near 80 K

frequencies were found to require different compressor-displacer phase relationships, the presented data are for optimized phase at each operating point; the optimum phase typically drops by 15 degrees as the frequency changes from 30 Hz to 50 Hz.

Figure 13 presents the measured sensitivity of various aspects of the cooler's thermal performance to drive frequency for a nominal 800-mW coldtip load at 80 K. Figure 13a shows the phase between the drive current and compressor piston position, and the compressor motor efficiency, given by⁷:

$$\eta_{\text{Motor}} = \frac{(\text{input electrical power} - i^2R)}{\text{input electrical power}} \quad (3)$$

In this expression (i) is the drive current and (R) is the drive coil resistance. Linear motors are most efficient when operating at resonance, and Fig. 13a clearly demonstrates this; note that the resonant frequency, indicated by the 90 degree phase, coincides with the maximum compressor motor efficiency.

In contrast to compressor motor efficiency, Fig. 13b illustrates the variation in overall cooler thermal efficiency (COP), as defined by:

$$\text{COP} = \frac{\text{cooling power}}{(\text{input electrical power} - i^2R)} \quad (4)$$

The optimum COP is seen to have its maximum near 35 Hz. Figure 13b also shows that the highest overall cooler efficiency is achieved as a compromise between compressor motor efficiency and thermal efficiency, and

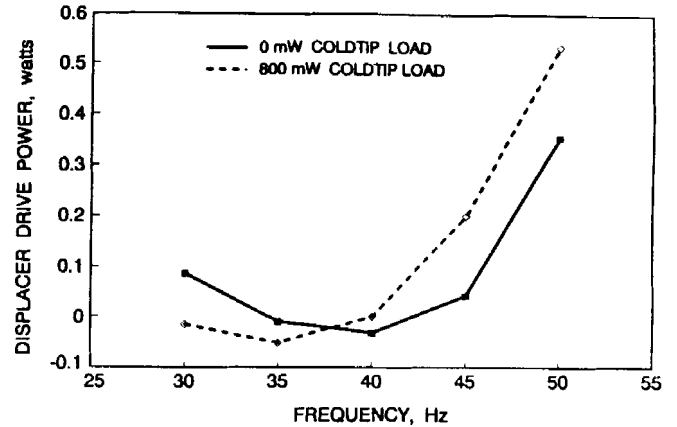


Fig. 14. Displacer drive power as a function of frequency for two different coldtip loads

reaches a maximum near 40 Hz.

Although the compressor draws significant electrical power during cooler operation, the displacer draws comparatively little electrical power; this is because its primary driving force is via pneumatic pressures from the compressor. Figure 14 shows the displacer electrical drive power as a function of frequency. Note that the displacer is also mechanically tuned to draw a minimum of power at drive frequencies near 40 Hz.

COMPRESSOR AND DISPLACER DC OFFSET- As a last sensitivity analysis it is instructive to examine the effect of moving the neutral position of the piston or displacer toward or away from the cylinder head so as to subtract or add dead volume to the compression space or cold expansion space, respectively. Because increased dead volume is known to be detrimental to thermal efficiency, it is of interest to quantify what efficiency improvements might accrue by using piston offset to minimize dead volume during periods when full stroke is not being used. Figure 15 presents the sensitivity of thermal performance for compressor dc offsets of -1 mm, 0 mm, and 1 mm. A negative offset corresponds to decreasing the dead volume in the compression space. It is estimated that a 1 mm offset changes the total active cooler volume by approximately 5%. Note that the

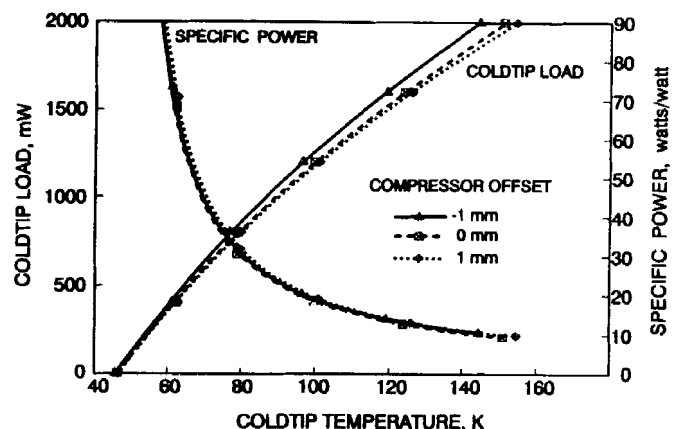


Fig. 15. Performance curves for compressor dc offsets of -1 mm, 0 mm, and 1 mm

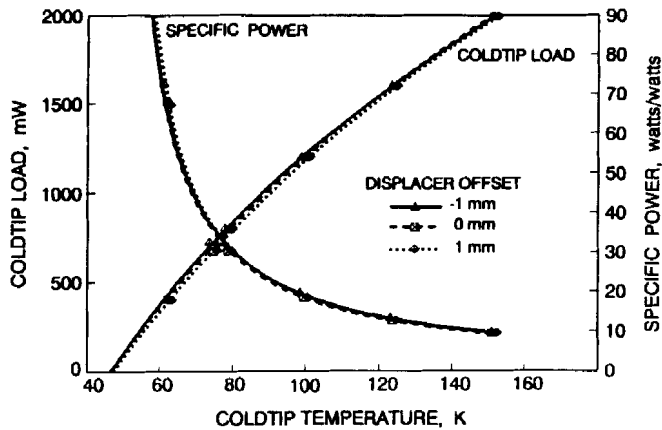


Fig. 16. Performance curves for displacer dc offsets of -1 mm, 0 mm, and 1 mm

cooling performance increases only slightly for decreasing dead volume, and the specific power shows only a small effect.

Figure 16 shows the performance for displacer dc offsets of -1 mm, 0 mm, and 1 mm; again, negative offset corresponds to reducing the cold-end dead volume. These offsets are substantial, as the dead volume change for a 1 mm offset corresponds to about 38% of the nominal displacer swept volume. However, the effect of the offset on performance is minimal. It was originally anticipated that there would be a significant increase in performance by reducing the cold-end dead volume, as this would reduce the mass flow through the regenerator and thus reduce the irreversibility due to regenerator inefficiency. However, we speculate that by shifting the neutral position of the displacer toward the cold end, the cold-space heat-transfer area and the effective length of the coldfinger is reduced, resulting in larger thermal conduction losses and counteracting any gain in performance.

SUMMARY

This study of the thermal performance of the BAe 80K cooler represents an important part of a broader characterization program underway at JPL to generate comprehensive test data on space cryocoolers for the space-instrument community. In addition to providing definitive performance data for the cooler user community, the stable test platform, excellent repeatability, and unique calorimetric methods used in this study are expected to prove to be equally effective for accurately quantifying important parameter sensitivities and design tradeoffs of interest to cooler developers.

The test measurements presented in this paper represent the most comprehensive characterization of the

thermal performance of the BAe 80K cooler that has been published to date. The performance, defined by the cooling power and specific power, has been mapped for a broad range of heat sink temperatures, compressor and displacer strokes, compressor-displacer phase, drive frequencies, and compressor and displacer dc offsets.

ACKNOWLEDGEMENT

The work described in this paper was carried out by the Jet Propulsion Laboratory, California Institute of Technology, under a contract with the National Aeronautics and Space Administration. Particular credit is due S. Leland, who manufactured and assembled much of the test setup, and E. Jetter who reduced much of the data to the graphs presented herein. The collaborative support of B. Jones of British Aerospace and the financial support of JPL's Eos-AIRS instrument are graciously acknowledged.

REFERENCES

1. R.G. Ross, Jr., D.L. Johnson, and R.S. Sugimura, "Characterization of Miniature Stirling-cycle Cryocoolers for Space Application," Proceedings of the 6th International Cryocooler Conference, Plymouth, MA, DTRC-91/002, David Taylor Research Center (1991), p. 27.
2. C.A. Lewis, "Long-life Stirling-cycle Coolers for Applications in the 60-110 K Range: Vibration Characterization and Thermal Switch Development," SAE Paper 891496, Society of Automotive Engineers, Warrendale, PA (1989).
3. R.G. Ross, Jr., D.L. Johnson, and V. Kotsubo, "Vibration Characterization and Control of Miniature Stirling-cycle Cryocoolers for Space Application," Adv. Cryo. Engin., vol. 37B (1991), p. 1019.
4. V. Kotsubo, D.L. Johnson, and R.G. Ross, Jr., "Cold-tip Off-state Conduction Loss of Miniature Stirling Cycle Cryocoolers," Adv. Cryo. Engin., vol. 37B (1991), p. 1037.
5. D.L. Johnson, and R.G. Ross, Jr., "Electromagnetic Compatibility Characterization of a BAe Stirling-cycle Cryocooler for Space Applications," Adv. Cryo. Engin., vol. 37B (1991), p. 1045.
6. W. Burt and R. Orsini, "Thermal Characterization of the BAe 80K Stirling Cycle Cooler," Adv. Cryo. Engin., vol. 37B (1991), p. 1069.
7. A.H. Orlowska and G. Davey, "Measurement of Losses in a Stirling-cycle Cooler," Cryogenics, vol. 27 (1987), p. 645.